PAPER

Inhibiting the shuttle effect in lithium–sulfur batteries using a layer-by-layer assembled ion-permselective separator†

Minsu Gu,[a] Jukyoung Lee,[a] Yongil Kim,[a] Joon Soo Kim,[b] Bo Yun Jang,*[b] Kyu Tae Lee*[a] and Byeong-Su Kim*[ac]

A novel strategy for introducing ion-permselective properties in a conventional polyethylene (PE) separator to inhibit the shuttle effect of polysulfides in high-performance lithium–sulfur batteries is reported. This was accomplished by taking advantage of the pH-responsive multilayers of weak polyelectrolytes such as poly(allylamine hydrochloride) (PAH) and poly(acrylic acid) (PAA) assembled on the PE separator using layer-by-layer (LbL) assembly. It was found that the cationic permselectivity (permeability of cation/anion) of an ultrathin multilayer coated separator is highly tunable with respect to the number of bilayers and external pH, benefiting from fine tuning of the internal charge density of the multilayered films. The movement of polysulfide anions was significantly inhibited by five bilayers of PAH/PAA (*ca.* 98% with multilayers assembled at pH 3/3), while the movement of Li cations was preserved. As a result, the ion-permselective separator demonstrated a high initial reversible capacity of *ca.* 1418 mA h g^{-1} with multilayers assembled at pH 3/3 because of the good permselectivity and the enhanced wetting properties of the LbL treated separator for electrolytes, leading to a significantly improved Coulombic efficiency as compared to a conventional PE separator, *i.e.*, almost 100% over 50 cycles. We anticipate that the permselectivity controllable coating method will be applied for various other membrane technologies.

Introduction

Increasing energy demands, coupled with the limited availability of fossil fuels and their associated environmental issues, have stimulated intense research on energy storage and conversion systems. Although lithium-ion batteries are the leading choice for energy storage today, they cannot sufficiently satisfy long-term storage requirements due to the inherent limitation of gravimetric energy density to meet various energy demands such as the transportation market and energy storage systems.[1] As one of the complements beyond lithium-ion batteries, lithium–sulfur (Li–S) batteries have recently received attention as promising power sources because of their remarkable theoretical specific capacity (1675 mA h g^{-1}) and energy density (2600 W h kg^{-1}), which are three to five times

higher than those of conventional lithium-ion batteries, together with the low cost of abundant sulfur.[2,3]

Despite these promising features, there are still some issues that need to be resolved, including the poor electronic conductivity of sulfur, dissolution of intermediate polysulfides, and large volume expansion (~80%).[4–6] In particular, the dissolved intermediate of polysulfides (Li$_2$S$_x$, 2 < x < 8) can diffuse from the cathode to the anode through the separator and this so-called "shuttle effect" can lead to rapid decay of the capacity and poor Coulombic efficiency during charging–discharging cycles. In that regard, there has been significant progress in improving these electrodes by using porous carbon,[7–9] hollow carbon spheres,[10–12] carbon nanotubes (CNT),[13–15] graphene oxide (GO),[16–22] conductive polymer coatings[23–25] and inorganic coatings[26–28] on sulfur particles. On the other hand, despite the separator also being critical to the performance of Li–S batteries, little research has been carried out on the separator. Some examples include, Manthiram and co-workers who reported that polysulfide can be trapped in a 3-dimensional carbon paper as an additional layer on the separator.[29,30] Liu and co-workers showed that lithiated Nafion ionomer separator film, which is used in proton exchange membrane fuel cells, can be applied to Li–S batteries.[31] Cheng and co-workers introduced a flexible sulfur–carbon nanotube cathode membrane without any metal current collector and binder.[32] Wei and co-workers

*a*Department of Energy Engineering, School of Energy and Chemical Engineering, Ulsan National Institute of Science and Technology (UNIST), 50 UNIST-gil, Ulsan 689-798, Korea. E-mail: ktlee@unist.ac.kr

*b*Korea Institute of Energy Research (KIER), Daejeon 305-343, Korea. E-mail: byjang@kier.re.kr

*c*Department of Chemistry, School of Natural Science, Ulsan National Institute of Science and Technology (UNIST), 50 UNIST-gil, Ulsan 689-798, Korea. E-mail: bskim19@unist.ac.kr

† Electronic supplementary information (ESI) available. See DOI: 10.1039/c4ra09718a

recently demonstrated a strategy of introducing an electrostatic shield using sulfonate (SO_3^-) groups of Nafion coating on the Celgard membrane.[33] In addition, composite gel polymer electrolyte has been used as a membrane, instead of separator, in Li–S batteries.[34–36] However, it is still highly desirable to improve the performance of conventional separators.

Alternatively, our approach in this study was to inhibit the shuttle effect of polysulfides by coating the conventional polyethylene (PE) separator with ion-permselective ultrathin films of polyelectrolytes using the layer-by-layer (LbL) assembly method. LbL deposition is a versatile thin film fabrication technique that forms multilayer thin films by depositing alternating layers of oppositely charged materials.[37,38] One of the advantages of using the LbL method is that it can easily control the composition and thickness of the nanoscale coating using a variety of materials of choice. Because of these unique features, LbL assembly has been applied to various membrane technologies such as proton exchange membrane fuel cells,[39] direct methanol fuel cells,[40–43] vanadium redox flow batteries,[44–46] Li–air batteries,[47] desalination,[48] and nanofiltration membranes.[49] Furthermore, LbL assembly allows for fine tuning of the internal charge density of multilayer films with changes in the external pH when weak polyelectrolytes such as poly(allylamine hydrochloride) (PAH) and poly(acrylic acid) (PAA) are employed.[50–52] For example, it is known that the degree of ionization of PAH ($pK_a \sim 9$) and PAA ($pK_a \sim 5$) is highly sensitive to the pH of the dipping solution which influences the relative fraction charged to uncharged group such as NH_3^+/NH_2 for PAH and $COO^-/COOH$ for PAA as well as the population of ionic bonds.
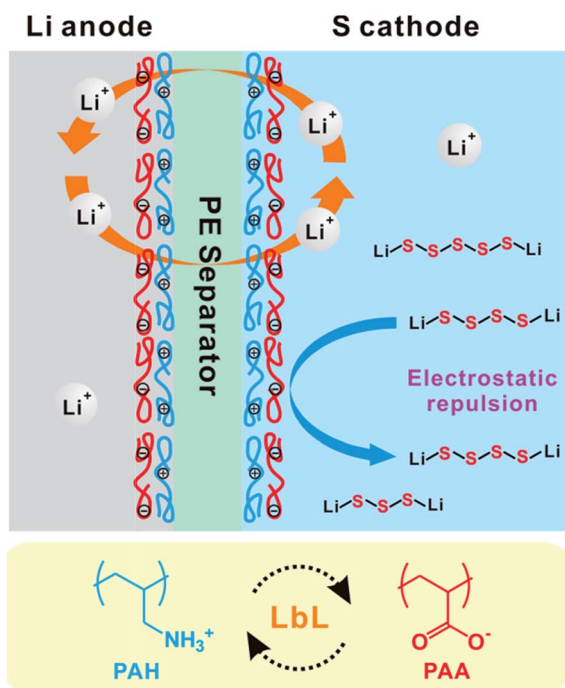
Herein, we fabricated an ion-permselective membrane on a conventional PE separator using LbL assembly to alleviate the shuttle effect of polysulfides in Li–S batteries (Scheme 1). This allows the positively charged Li-ion to freely diffuse through the separator, whereas the movement of the negatively charged polysulfide will be inhibited by due to the electrostatic repulsion of the ion-permselective multilayer films bearing large amounts of carboxylic acid groups.

Experimental

Layer-by-layer assembly of (PAH/PAA)$_n$ multilayer coated separator

A PE separator (4.5 cm × 8.0 cm) was treated with oxygen plasma (Harrick plasma, PDC-32G) for 1 min to introduce a hydrophilic surface. The PE separator was dipped in a positively charged PAH solution (Sigma-Aldrich, $M_w \sim 15\,000$, 5 mg mL^{-1}) at each pH condition for 10 min. It was then dipped into DI water at the same pH condition three times for 1 min each. Subsequently, the PE separator was dipped in a negatively charged PAA solution (Sigma-Aldrich, $M_w \sim 250\,000$, 5 mg mL^{-1}) at each adjusted pH condition for 10 min, and washed with DI water at the same pH condition three times for 1 min, affording one-bilayer of (PAH/PAA)$_1$. The above procedures were repeated to achieve the desired number of bilayers (typically, $n = 1$–9). These as-assembled (PAH/PAA)$_n$ multilayer coated PE separators were dried at room temperature.

Cell assembly and electrochemical test

The active materials were composed of CMK-3 and sulfur at 50 : 50 weight ratios. Samples of electrochemically active materials were mixed with carbon black and polyvinylidene fluoride (PVdF) at 80 : 10 : 20 weight ratios. These as-prepared active materials were loaded on an Al foil current collector. The Li ion cells were assembled in an argon-filled glove box. The electrochemical performance of the Li ion batteries was evaluated using 2032 coin cells (Hohsen Co., Japan), with a Li metal anode and 1.3 M lithium bis(trifluoromethanesulfonyl)imide (LiTFSI) in tetraethylene glycol dimethyl ether (TEGDME) electrolyte solution. LbL coated PE film was used as a separator. Galvanostatic experiments were performed in the voltage range of 1.5 to 2.6 V at a 0.05 C-rate and a temperature of 30 °C.

Ion-permselective property test

Cyclic voltammetry (CV) measurements were performed according to the literature.[52] A three-electrode cell was used at a scan rate of 100 mV s^{-1}. The PAH/PAA multilayer coated ITO glasses at each pH were used as the working electrodes. A platinum wire was used as a counter electrode, and Ag/AgCl (3.0 M NaCl) was used as a reference electrode. The electrolyte solution was prepared by adding 5 mM of either $Fe(CN)_6^{3-}$ or $Ru(NH_3)_6^{3+}$ to 0.50 M Na_2SO_4 at pH 6. The measured current was divided by the area of the ITO electrode immersed in electrolyte solution (in our case 1.05 cm^2) to obtain the current density value.

Scheme 1 Schematic representation of layer-by-layer (LbL) assembled (PAH/PAA)$_n$ multilayer coated PE separator for inhibiting the shuttle effect of polysulfide across the separator in a Li–S battery.

Characterizations

Attenuated total reflectance-infrared (ATR-IR) spectra were analyzed with a FT-IR spectrophotometer (Varian, 670-IR). The surface morphology of the samples was investigated using a scanning electron microscope (FESEM, FEI, Nanonova 230). The contact angle was obtained using a contact angle analyzer (KRÜSS, DSA 100). The thickness of the as-prepared samples on the silicon substrates was measured by ellipsometry (J. A. Woollam Co. Inc., EC-400 and M-2000V).

Results and discussion

Since both polymers employed in this study are weak polyelectrolytes, we investigated the assembly of PAH and PAA polyelectrolytes based on three different conditions in this study, namely pH 3/3, 6/3, and 8.5/8.5 for PAH/PAA. Initially, we monitored the stepwise fabrication of PAH/PAA multilayer films on a silicon wafer by using a spectroscopic ellipsometry. As shown in Fig. 1a, the growth of the $(PAH/PAA)_n$ is linear with respect to the number of bilayers in both pH 3/3 and 8.5/8.5 conditions; however, it becomes exponential in the case of the pH 6/3 condition. It was found that the average thickness of one bilayer of (PAH/PAA) film corresponds to 3.6 nm (pH 3/3), 20.1 nm (pH 6/3), and 2.1 nm (pH 8.5/8.5), respectively. Similar to other reported systems, the assembly pH of each polymer is critical in determining the final thickness and composition of the resulting multilayers; for example, when both PAH and PAA are deposited at pH 3/3, the PAH is fully ionized while PAA is

ionized less than 1% considering its pK_a value of ∼5. Thus, the loopy PAA chains that contain a large amount of free carboxylic acid groups make complexes with example, PAA is now fully ionized (more than 60%) while the degree of ionization in the PAH chain is modestly diminished. Therefore, PAH adsorbs tightly onto the highly ionized PAA surface chains, forming a thinner layer. On the other hand, the pH 6/3 condition, moderately charged PAH alternated with partially charged PAA polymers, yields the thickest films. This is because the pH of the dipping solution not only affects the ionization of polyelectrolytes in solution, but it also changes the ionization of the polyelectrolytes multilayers on which adsorption occurs. Specifically, the pre-adsorbed PAA chains undergo a drastic charge density increase when the pH changed from 3 to 6, which in turn recruit more PAH chains to compensate for the increased charge density of the PAA chains, eventually leading to the formation of the thickest bilayers with an exponential growth behavior.

Once we confirmed the successful fabrication of multilayer films, we fabricated $(PAH/PAA)_n$ multilayers on the conventional PE separator at three different pH conditions. In order to enhance the wettability of the conventional hydrophobic PE membrane, the PE separator was initially subjected to oxygen plasma treatment for 1 min. The oxygen plasma treatment changed the contact angle of a water droplet on the surface of PE from 119° to 87°. In addition, it was observed that the oxygen plasma treatment did not significantly damage the surface structure of PE separator under scanning electron microscopy (SEM) (Fig. S1†). Attenuated total reflectance-infrared (ATR-IR) spectroscopy was employed to monitor the characteristic peaks of the multilayer coated PE corresponding to the functional groups present in the polyelectrolytes as in Fig. 2. Five bilayer films of $(PAH/PAA)_5$ coated PE separator all showed the characteristic peaks of the PE separator with a scissoring band of the methylene ($-CH_2-$) backbone of PE at 1462 and 1473 cm^{-1}. the C=O stretching vibration peaks of carboxylic
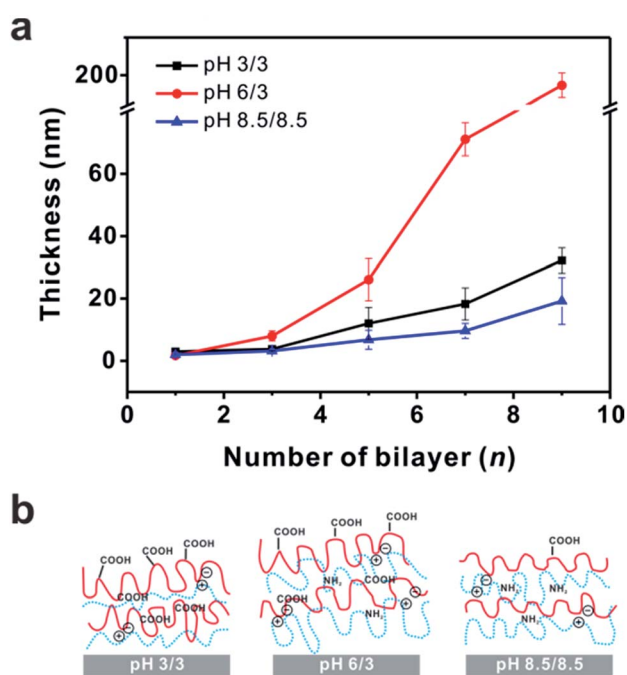
Fig. 1 (a) Thickness growth curve of the $(PAH/PAA)_n$ multilayer thin films on a silicon wafer with respect to the assembly pH conditions and (b) schematic representation of the internal structure of $(PAH/PAA)_n$ multilayer thin films assembled at different pH conditions. Thickness was measured in five independent measurements with ellipsometry.
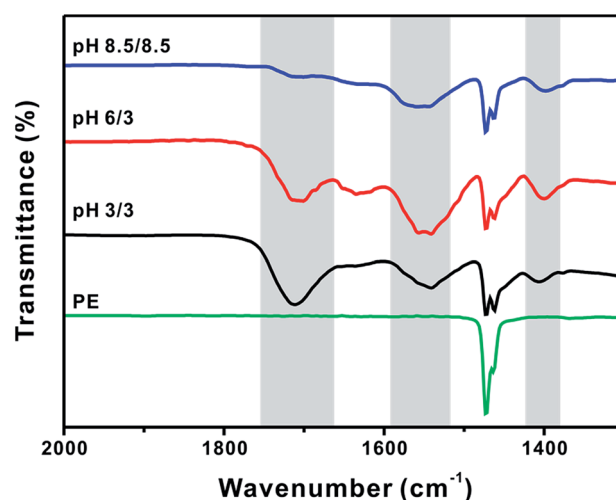
Fig. 2 ATR-IR spectra of $(PAH/PAA)_5$ multilayer coated PE-separator at each assembly pH.

acid ($-COOH$) at 1712 cm^{-1} and carboxylate ($-COO^-$) peaks at 1541 cm^{-1} and 1400 cm^{-1}. As expected, the transition from carboxylic acid groups to the carboxylate of PAA is well observed with increasing pH of the dipping solution. For instance, according to the peak intensity in the IR spectra, the relative fraction of carboxylate (COO^-) to carboxylic acid ($COOH$) at pH 3/3, 6/3, and 8.5/8.5 was determined to be 0.5, 1.31 and 3.33, respectively. This distinctly proved that the pH sensitive behavior of PAH/PAA multilayer films affect the LbL architecture, as shown in previous thickness growth curve (Fig. 1).

On the basis of the stable coating of the polyelectrolytes on the PE separator, we studied the surface morphology of the PE separator with a different number of bilayers that are assembled at respective pH conditions using a scanning electron microscopy (SEM) in Fig. 3. The first few layers of the polyelectrolyte coatings were hard to discern clearly due to the low contrast, yet we found that bare PE separators with a unique network of interconnected large pores were present. With increasing the number of bilayers, however, the pores of the bare PE separator were gradually blocked by the coated $(PAH/PAA)_n$ multilayer films. In particular, the pores of the PE separator were almost completely blocked by the thickest films of $(PAH/PAA)_5$ assembled at pH 6/3 in accord with the previous results of thickness measurements. Moreover, the surface property of the multilayer coated PE was also investigated with contact angle measurements, which revealed the internal composition of the polyelectrolytes within the multilayers. This is because the underlying layer of the LbL films is known to influence the surface property of films in concert with the previous literature of $(PAH/PAA)_n$ multilayer systems.[53] As a result, the PAH-rich multilayers displayed a more hydrophobic surface, as evidenced by the high pH assembly conditions of pH 8.5/8.5, whereas PAA-rich multilayers retained a more hydrophilic surface in the film assembled at pH 3/3 condition. On the other

hand, because the segments of PAH and PAA are present in a similar amount in the case of pH 6/3, contact angle decreased at initial stage but increased gradually because of the exponential growth of the LbL films and enhanced surface roughness. These results are in good agreement with previous reports on which how different assembly conditions can lead to the internal structure of polyelectrolytes multilayers and their modified thin films.[50]

To evaluate the ion-permselectivity of the multilayers that are assembled at different pH conditions, we used two different charged redox probe molecules, such as cationic $Ru(NH_3)_6^{3+}$ and anionic $Fe(CN)_6^{3-}$, respectively. Cyclic voltammogram (CV) analysis was carried out using $(PAH/PAA)_n$ multilayer coated ITO glass at pH 3/3. As shown in Fig. 4, the cationic charge probe, $Ru(NH_3)_6^{3+}$, can penetrate through the PAH/PAA films, but the current density diminished marginally with the increase of film thickness because of the limited diffusion of the small molecule through the polyelectrolyte multilayers (ca. 15% with 5 BL film). In clear contrast, the movement of the anionic probe, $Fe(CN)_6^{3-}$, is significantly inhibited by the $(PAH/PAA)_n$ films, indicating a 72% decrease in current density even at 1 BL film and decreases further with growth of the $(PAH/PAA)_n$ films (ca. 98% with 5 BL). This observation can be explained by the following. At pH 3/3, PAA containing free carboxyl acid groups is adsorbed on fully ionized PAH. If this LbL film is dipped in a neutral solution above the pK_a of PAA, the many free carboxyl acid groups of PAA are deprotonated, forming carboxylate groups. As a result, the internal charge density of the $(PAH/PAA)_5$ films becomes considerably more negative, which repels anionic probe molecules like $Fe(CN)_6^{3-}$. This cation-
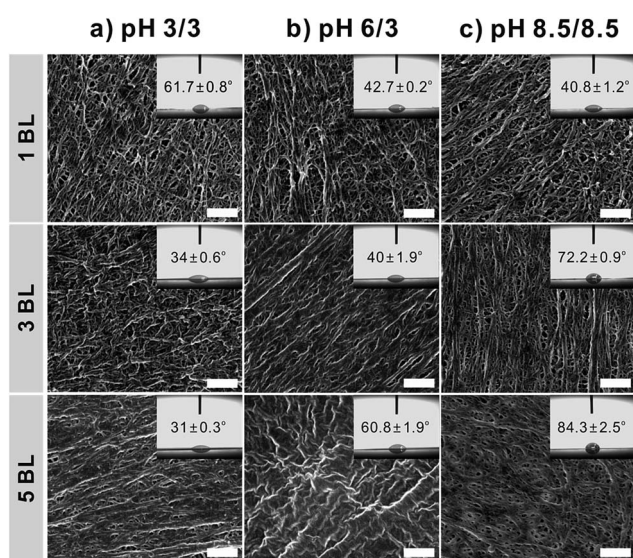
Fig. 3 SEM images of PAH/PAA 1, 3, and 5 bilayer (BL) coated on separator by LbL assembly at (a) pH 3/3, (b) pH 6/3 and (c) pH 8.5/8.5. The scale bar of each image is 1 μm.
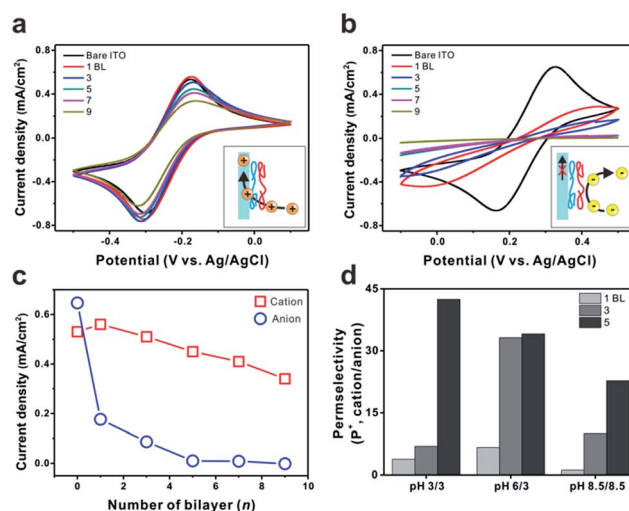
Fig. 4 Cyclic voltammograms (CV) of $(PAH/PAA)_n$ multilayer of pH 3/3 coated on ITO glass by LbL assembly in an aqueous 0.50 M Na$_2$SO$_4$ electrolyte solution containing 5.0 mM of (a) $Ru(NH_3)_6^{3+}$ as the cationic and (b) $Fe(CN)_6^{3-}$ as the anionic probes, respectively. Inset image shows the schematic representation of the cation exchange property of LbL thin films. (c) The comparison of anodic peak current density of each ion species. (d) Calculated permselectivity, P^+, (selectivity ratio of cation to anion) with different numbers of bilayers and pH conditions.

exchangeable property was also seen at pH 6/3 and pH 8.5/8.5, but the amount of negative charges in the LbL films was different (Fig. S2†). Cationic retention (I^+/I_o^+, where I^+ is current density at each condition, and I_o^+ is current density on bare electrode of cation) of 5 BL at pH 3/3, 6/3, and 8.5/8.5 was maintained at 85%, 47%, and 59%, respectively, (Fig. S3a†), while anionic retention (I^-/I_o^-, where I^- is current density at each condition, and I_o^- is current density on bare electrode of anion) noticeably decreased to 2%, 1.4%, and 2.6%, respectively, with 5 BL (Fig. S3b†). In other words, LbL multi-layer coating has an ion-permselective property similarly observed in other works,[52,54] and our system is only cation-exchangeable. Furthermore, we calculated the cationic permselectivity (P^+) under different conditions using a simple eqn (1).

$$P^+ = \frac{I^+/I_o^+}{I^-/I_o^-} \tag{1}$$

As a result, cationic permselectivity increased at all of the pH conditions with respect to the number of bilayers. However, pH 3/3 showed the best ion-permselective property (pH 3/3 > pH 6/3 > pH 8.5/8.5), which corresponds to the amount of free carboxyl acid groups in PAA.

The electrochemical performance of CMK-3/S using bare PE and (PAH/PAA)$_5$ coated PE separators at each pH were compared (Fig. 5). Note that any additive such as lithium nitrate forming stable passivation films on Li metal was not used to evaluate the inherent effect of separators on the shuttle phenomena of dissolved polysulfides, because it is well-known that stable passivation layers on Li itself inhibit the shuttle effect. The key parameter determining the appearance of the shuttle effect is Columbic efficiency which was defined as the ratio of discharge capacity to charge capacity, because charge capacity surpasses the discharge capacity when dissolved polysulfides cause self-discharges (shuttle effect). Remarkably, all of the LbL treated separators show highly improved Coulombic efficiencies with almost 100%, which means the shuttle effect of polysulfide is effectively inhibited, which is shown by comparing each pH to the bare PE separator in Fig. 5c. The Coulombic efficiency of the bare PE separator was 59% at minimum and 69% after 50 cycles. However, pH 3/3, pH 6/3 and pH 8.5/8.5 maintain the Coulombic efficiency with 98%, 104%, and 99%, respectively. This clearly demonstrated that the ion-permselective LbL thin film coating on the PE separator effectively inhibited the movement of the dissolved polysulfides from the cathode to anode in Li–S batteries. The CMK-3/S electrodes with the bare PE separator and PAH/PAA coated separators at pH 3/3, and 8.5/8.5 delivered high reversible capacities of ca. 1302, 1418, and 1350 mA h g^{-1} at the first cycle, respectively (Fig. 5d), indicating Li$^+$ ion conduction through both the bare and PAH/PAA coated separators is fast enough because of the good wetting property of both separators for electrolytes. However, the reversible capacity of pH 6/3 was significantly lower than that of any other cases, which is attributed to the fact that Li ions cannot diffuse into the separator because the pores of the separator were clogged by the densely packed coating layers as shown in Fig. 3b. In addition, owing to the inhibited shuttle effect of the coated separators, the pH 3/3 and 8.5/8.5 conditions showed better cycle performance than the bare separator (Fig. 5d). Moreover, the pH 3/3 exhibited slightly better capacity retention than the 8.5/8.5. This is attributed to that the amount of loaded PAA on the pH 3/3 LbL film is much higher than that of PAH, and the charge of LbL film is also highly negative. The negatively charged intensity of the pH 8.5/8.5 LbL film is relatively weaker because of the smaller amount of COOH of in the PAA chains than at pH 3/3 condition.

Conclusions

In conclusion, we have developed a simple method of constructing polymer coated separators by nanoscale thin film coating LbL assembly. The separator prepared by the LbL method offers precise control not only over the thickness of the coating films, but also the charge density of the whole films by changing the number of bilayers as well as external pH conditions (pH 3/3, 6/3, and 8.5/8.5) that can control the relative fraction of charged carboxylate group over non-charged carboxylic acid group. Especially, the case of pH 3/3, which has large amount of free carboxyl acid groups in PAA, showed the best cationic permselectivity, necessary for inhibiting the shuttle effect. As a result, ion-permselective separators showed the enhanced Coulombic efficiency reaching almost 100% and cycle performance of Li–S batteries. This study introduces a new strategy for creating the separator in Li–S batteries that can decrease the migration of soluble high-order Li–polysulfide (Li$_2$S$_3$ to Li$_2$S$_6$) from the cathode to the anode through the separator.

Fig. 5 Voltage profiles of the (a) bare PE separator and (b) (PAH/PAA)$_5$ coated PE separator at pH 3/3. (c) Cycle performance and (d) Coulombic efficiency of the (PAH/PAA)$_5$ coated separator at each pH and comparison to bare PE separator.

Acknowledgements

Notes and references

1 P. G. Bruce, S. A. Freunberger, L. J. Hardwick and J. M. Tarascon, *Nat. Mater.*, 2012, **11**, 19–29.
2 N.-S. Choi, Z. Chen, S. A. Freunberger, X. Ji, Y.-K. Sun, K. Amine, G. Yushin, L. F. Nazar, J. Cho and P. G. Bruce, *Angew. Chem., Int. Ed.*, 2012, **51**, 9994–10024.
3 M.-K. Song, E. J. Cairns and Y. Zhang, *Nanoscale*, 2013, **5**, 2186–2204.
4 Y. Yang, G. Y. Zheng and Y. Cui, *Chem. Soc. Rev.*, 2013, **42**, 3018–3032.
5 S. Evers and L. F. Nazar, *Acc. Chem. Res.*, 2013, **46**, 1135–1143.
6 D.-W. Wang, Q. Zeng, G. Zhou, L. Yin, F. Li, H.-M. Cheng, I. R. Gentle and G. Q. M. Lu, *J. Mater. Chem. A*, 2013, **1**, 9382–9394.
7 X. Ji, K. T. Lee and L. F. Nazar, *Nat. Mater.*, 2009, **8**, 500–506.
8 G. Zheng, Q. Zhang, J. J. Cha, Y. Yang, W. Li, Z. W. Seh and Y. Cui, *Nano Lett.*, 2013, **13**, 1265–1270.
9 S. Moon, Y. H. Jung, W. K. Jung, D. S. Jung, J. W. Choi and D. K. Kim, *Adv. Mater.*, 2013, **25**, 6547–6553.
10 J. Schuster, G. He, B. Mandlmeier, T. Yim, K. T. Lee, T. Bein and L. F. Nazar, *Angew. Chem., Int. Ed.*, 2012, **51**, 3591–3595.
11 C. Zhang, H. B. Wu, C. Yuan, Z. Guo and X. W. Lou, *Angew. Chem., Int. Ed.*, 2012, **51**, 9592–9595.
12 S. Xin, Y.-X. Yin, L.-J. Wan and Y.-G. Guo, *Part. Part. Syst. Charact.*, 2013, **30**, 321–325.
13 L. Wang, Z. Dong, D. Wang, F. Zhang and J. Jin, *Nano Lett.*, 2013, **13**, 6244–6250.
14 Y. Fu, Y.-S. Su and A. Manthiram, *Angew. Chem., Int. Ed.*, 2013, **52**, 6930–6935.
15 J.-H. Choi, C.-L. Lee, K.-S. Park, S.-M. Jo, D.-S. Lim and I.-D. Kim, *RSC Adv.*, 2014, **4**, 16062–16066.
16 S. Lu, Y. Chen, X. Wu, Z. Wang and Y. Li, *Sci. Rep.*, 2014, **4**, 4629–4632.
17 J. Rong, M. Ge, X. Fang and C. Zhou, *Nano Lett.*, 2014, **14**, 473–479.
18 S. Lu, Y. Cheng, X. Wu and J. Liu, *Nano Lett.*, 2013, **13**, 2485–2489.
19 M. Xiao, M. Huang, S. Zeng, D. Han, S. Wang, L. Sun and Y. Meng, *RSC Adv.*, 2013, **3**, 4914–4916.
20 H. Wang, Y. Yang, Y. Liang, J. T. Robinson, Y. Li, A. Jackson, Y. Cui and H. Dai, *Nano Lett.*, 2011, **11**, 2644–2647.
21 L. W. Ji, M. M. Rao, H. M. Zheng, L. Zhang, Y. C. Li, W. H. Duan, J. H. Guo, E. J. Cairns and Y. G. Zhang, *J. Am. Chem. Soc.*, 2011, **133**, 18522–18525.
22 W. Li, Q. Zhang, G. Zheng, Z. W. Seh, H. Yao and Y. Cui, *Nano Lett.*, 2013, **13**, 5534–5540.
23 Y. Yang, G. H. Yu, J. J. Cha, H. Wu, M. Vosgueritchian, Y. Yao, Z. A. Bao and Y. Cui, *ACS Nano*, 2011, **5**, 9187–9193.
24 L. Xiao, Y. Cao, J. Xiao, B. Schwenzer, M. H. Engelhard, L. V. Saraf, Z. Nie, G. J. Exarhos and J. Liu, *Adv. Mater.*, 2012, **24**, 1176–1181.
25 M. Wang, W. Wang, A. Wang, K. Yuan, L. Miao, X. Zhang, Y. Huang, Z. Yu and J. Qiu, *Chem. Commun.*, 2013, **49**, 10263–10265.
26 Z. W. Seh, W. Li, J. J. Cha, G. Zheng, Y. Yang, M. T. McDowell, P.-C. Hsu and Y. Cui, *Nat. Commun.*, 2013, **4**, 1331–1336.
27 K. T. Lee, R. Black, T. Yim, X. Ji and L. F. Nazar, *Adv. Energy Mater.*, 2012, **2**, 1490–1496.
28 J. Y. Li, B. Ding, G. Y. Xu, L. R. Hou, X. G. Zhang and C. Z. Yuan, *Nanoscale*, 2013, **5**, 5743–5746.
29 C. Zu, Y.-S. Su, Y. Fu and A. Manthiram, *Phys. Chem. Chem. Phys.*, 2013, **15**, 2291–2297.
30 S.-H. Chung and A. Manthiram, *Chem. Commun.*, 2014, **50**, 4184–4187.
31 Z. Jin, K. Xie, X. Hong, Z. Hu and X. Liu, *J. Power Sources*, 2012, **218**, 163–167.
32 G. Zhou, D.-W. Wang, F. Li, P.-X. Hou, L. Yin, C. Liu, G. Q. Lu, I. R. Gentle and H.-M. Cheng, *Energy Environ. Sci.*, 2012, **5**, 8901–8906.
33 J. Q. Huang, Q. Zhang, H. J. Peng, X. Y. Liu, W. Z. Qian and F. Wei, *Energy Environ. Sci.*, 2014, **7**, 347–353.
34 J. Hassoun and B. Scrosati, *Angew. Chem., Int. Ed.*, 2010, **49**, 2371–2374.
35 J. Jin, Z. Y. Wen, X. Hang, Y. M. Cui and X. W. Wu, *Solid State Ionics*, 2012, **225**, 604–607.
36 S. S. Zhang, *J. Electrochem. Soc.*, 2013, **160**, A1421–A1424.
37 G. Decher, *Science*, 1997, **277**, 1232–1237.
38 J. Hong, J. Y. Han, H. Yoon, P. Joo, T. Lee, E. Seo, K. Char and B.-S. Kim, *Nanoscale*, 2011, **3**, 4515–4531.
39 T. Tago, H. Shibata and H. Nishide, *Chem. Commun.*, 2007, 2989–2991.
40 A. A. Argun, J. N. Ashcraft and P. T. Hammond, *Adv. Mater.*, 2008, **20**, 1539–1543.
41 J. N. Ashcraft, A. A. Argun and P. T. Hammond, *J. Mater. Chem.*, 2010, **20**, 6250–6257.
42 D. S. Liu, J. N. Ashcraft, M. M. Mannarino, M. N. Silberstein, A. A. Argun, G. C. Rutledge, M. C. Boyce and P. T. Hammond, *Adv. Funct. Mater.*, 2013, **23**, 3087–3095.
43 H. Deligoz, S. Yilmazturk, T. Karaca, H. Ozdemir, S. N. Koc, F. Oksuzomer, A. Durmus and M. A. Gurkaynak, *J. Membr. Sci.*, 2009, **326**, 643–649.
44 J. Xi, Z. Wu, X. Teng, Y. Zhao, L. Chen and X. Qiu, *J. Mater. Chem.*, 2008, **18**, 1232–1238.
45 C. Jia, J. Liu and C. Yan, *J. Power Sources*, 2012, **203**, 190–194.
46 W. Xu, X. Li, J. Cao, H. Zhang and H. Zhang, *Sci. Rep.*, 2014, **4**, 4016–4024.
47 S. H. Lee, J. R. Harding, D. S. Liu, J. M. D'Arcy, Y. Shao-Horn and P. T. Hammond, *Chem. Mater.*, 2014, **26**, 2579–2585.
48 J. Park, J. Park, S. H. Kim, J. Cho and J. Bang, *J. Mater. Chem.*, 2010, **20**, 2085–2091.
49 Y. Cho, J. Lim and K. Char, *Soft Matter*, 2012, **8**, 10271–10278.
50 S. S. Shiratori and M. F. Rubner, *Macromolecules*, 2000, **33**, 4213–4219.

51 J. D. Mendelsohn, C. J. Barrett, V. V. Chan, A. J. Pal, A. M. Mayes and M. F. Rubner, *Langmuir*, 2000, **16**, 5017–5023.

52 M. K. Park, S. X. Deng and R. C. Advincula, *J. Am. Chem. Soc.*, 2004, **126**, 13723–13731.

53 D. Yoo, S. S. Shiratori and M. F. Rubner, *Macromolecules*, 1998, **31**, 4309–4318.

54 Q. Li, J. F. Quinn and F. Caruso, *Adv. Mater.*, 2005, **17**, 2058–2062.